

Nucleon Decay as a Probe of Flavor Symmetry: The Case of Fake Unification

Masahiro Ibe^{a,b}, Satoshi Shirai^b and Keiichi Watanabe^a

^a *ICRR, The University of Tokyo, Kashiwa, Chiba 277-8582, Japan*

^b *Kavli Institute for the Physics and Mathematics of the Universe (WPI),
The University of Tokyo Institutes for Advanced Study,
The University of Tokyo, Kashiwa 277-8583, Japan*

Abstract

This paper explores nucleon decay within the framework of a “fake Grand Unified Theory (GUT)” combined with the Froggatt-Nielsen (FN) mechanism. In this fake GUT framework, quarks and leptons may have distinct high-energy origins but fit into complete $SU(5)$ multiplets at low energies without requiring force unification, setting it apart from conventional GUTs. By introducing flavor symmetry through the FN mechanism, the model addresses the flavor puzzle of quark and lepton mass hierarchies and mixing patterns. Our analysis demonstrates that nucleon decay rates and branching fractions in the fake GUT are sensitive to flavor symmetry, providing a means to distinguish it from conventional GUT predictions. These findings underscore the importance of nucleon decay searches in probing both baryon number violation and the underlying flavor structure.

1 Introduction

The Standard Model (SM) is remarkably successful due to its precise predictions across fundamental interactions, many of which have been experimentally confirmed. However, there remains the question of why quarks and leptons possess specific gauge representations. Interestingly, the matter fields of the SM have gauge representations that can be neatly embedded into the $\bar{\mathbf{5}}$ and $\mathbf{10}$ representations of $SU(5)$. Grand Unified Theory (GUT) is a framework which can explain this apparent matter unification by embedding the SM gauge groups into the $SU(5)$ gauge group. Consequently, the study of the GUT has been a long-standing pursuit [1–3] (see Ref. [4] for reviews). The GUT predicts nucleon decay, which is being extensively searched for across a variety of current and future experiments. (see e.g., Refs. [5–8]).

To explain the apparent matter unification, however, the force unification of the SM is not mandatory. In fact, the framework called “fake GUT” has been proposed as an alternative to explain the unification of SM matter into the $SU(5)$ multiplets without force unification [9, 10] (see also Refs. [11, 12] for related discussions within the $SO(10)$ GUT model). In this framework, quarks and leptons may have distinct origins at high energies although they automatically fit into complete $SU(5)$ multiplets at low energies. This approach helps address challenges faced by conventional GUT models, such as too rapid proton decay, failure to achieve successful gauge coupling unification, or difficulty in unifying quark and lepton Yukawa couplings. A notable aspect of the fake GUT is its ability to yield predictions for nucleon decay that vary significantly based on the flavor structure of the matter fields, as discussed in Ref. [10].

The flavor puzzle is another question that cannot be explained within the SM. This puzzle encompasses unresolved questions regarding the mass hierarchy of quarks and leptons, the specific structure of the CKM matrix, and flavor mixing of neutrinos. It remains quite puzzling that, although there is no distinction between the three generations of fermions from the perspective of gauge interactions, their Yukawa interactions exhibit significant differences. To address these issues, various flavor models have been proposed in addition to the GUT framework.

To explain the above flavor structures, various models and ideas have been proposed (see e.g., Refs. [13, 14] for reviews). Among these, the Froggatt-Nielsen (FN) mechanism provides a simple approach which can solve the flavor puzzle by utilizing the $U(1)$ symmetry and its subsequent breaking [15]. With appropriate $U(1)$ charge assignments of the SM fermions, hierarchical effective Yukawa interactions can be achieved from featureless Yukawa interactions where the fundamental dimensionless couplings are of order unity. This framework also allows for the reproduction of the observed mixing patterns across generations.

In this paper, we analyze the nucleon decay in the fake GUT with FN mechanism. As we will demonstrate, the nucleon decay rate and its branching fractions are sensitive to flavor symmetry in the fake GUT scenario. This contrasts sharply with nucleon decay mediated by GUT gauge bosons in conventional GUT models, where decay characteristics remain largely unaffected by flavor

symmetry. This feature highlights the experimental potential to differentiate between fake GUT and conventional GUT models in experiments such as Super-Kamiokande (SK), Hyper-Kamiokande (HK), JUNO, and DUNE experiments [5–8]. Additionally, these nucleon decay experiments offer a unique opportunity to probe aspects of flavor symmetry.

The organization of this paper is as follows. We first summarize the concrete fake GUT model based on $SU(5) \times U(2)_H$ in Ref. [10] in Sec. 2. In Sec. 3, we introduce the FN mechanism, and we examine several FN charge assignments that successfully reproduce the flavor structure of the SM in the fake GUT model. In Sec. 4, we investigate the nucleon decay in the $SU(5) \times U(2)_H$ model with the FN mechanism. In the final section, we present our conclusions.

2 Fake GUT Model Based on $SU(5) \times U(2)_H$

In this section, we summarize a minimal fake GUT model based on $G = SU(5) \times U(2)_H \simeq SU(5) \times SU(2)_H \times U(1)_H$ in Ref. [10]. Specifically, we provide a brief overview of the origin of SM fermions and Yukawa interactions, as well as key features of proton decay.

2.1 Origin of SM fermions

In this model, there are three generations of chiral fermions $\bar{\mathbf{5}} \oplus \mathbf{10}$ of $SU(5)$, and three pairs of vector-like fermions charged under $U(2)_H$ as follows:¹

$$\bar{\mathbf{5}} : (\bar{\mathbf{5}}, \mathbf{1})_0 \times 3, \quad \mathbf{10} : (\mathbf{10}, \mathbf{1})_0 \times 3, \quad (2.1)$$

$$[L_H : (\mathbf{1}, \mathbf{2})_{-1/2}, \quad \bar{L}_H : (\mathbf{1}, \mathbf{2})_{+1/2}] \times 3, \quad (2.2)$$

$$[E_H : (\mathbf{1}, \mathbf{1})_{-1}, \quad \bar{E}_H : (\mathbf{1}, \mathbf{1})_{+1}] \times 3. \quad (2.3)$$

Here, group representations are denoted by $(SU(5), SU(2)_H)_{U(1)_H}$. As discussed later, while the SM quark sector originates fully from $\bar{\mathbf{5}} \oplus \mathbf{10}$, the SM lepton sector is derived from a linear combination of $\bar{\mathbf{5}}(\mathbf{10})$ and $L_H(\bar{E}_H)$.

The spontaneous breaking of $SU(5) \times U(2)_H$ into $G_{\text{SM}} = SU(3)_c \times SU(2)_L \times U(1)_Y$ is achieved by a vacuum expectation value (VEV) of a complex scalar field ϕ_2 , which is in the bi-fundamental representation, $(\mathbf{5}, \mathbf{2})_{-1/2}$. Explicitly, the VEV of ϕ_2 is given by

$$\langle \phi_2 \rangle = \begin{pmatrix} 0 & 0 & 0 & v_2 & 0 \\ 0 & 0 & 0 & 0 & v_2 \end{pmatrix}, \quad (2.4)$$

which breaks $SU(5) \times U(2)_H$ down to G_{SM} . Here, v_2 is a scale associated with the fake GUT, much larger than the electroweak scale. In this case, $SU(3)_c$ remains as an unbroken subgroup of $SU(5)$, while $SU(2)_L$ and $U(1)_Y$ appear as diagonal subgroups of $SU(5)$ and $U(2)_H$. Additionally, $\bar{\mathbf{5}}$ and $\mathbf{10}$ decompose as follows:

$$\bar{\mathbf{5}} \rightarrow \bar{d}_{\text{SM}} \oplus L_{\bar{\mathbf{5}}}, \quad \mathbf{10} \rightarrow Q_{\text{SM}} \oplus \bar{u}_{\text{SM}} \oplus \bar{E}_{\mathbf{10}}. \quad (2.5)$$

¹In this paper, we use Weyl fermion notation throughout.

In this model, SM leptons come from massless linear combinations of $L_{\bar{\mathbf{5}}}(\bar{E}_{\mathbf{10}})$ and $L_H(\bar{E}_H)$. To illustrate this point explicitly, let us consider the following interactions between the fermions and ϕ_2 ,

$$\mathcal{L} = m_{L,ij} \bar{L}_{Hi} L_{Hj} + \lambda_{L,ij} \bar{L}_{Hi} \phi_2 \bar{\mathbf{5}}_j + m_{E,ij} E_{Hi} \bar{E}_{Hj} + \frac{\lambda_{E,ij}}{\Lambda_{\text{cut}}} E_{Hi} \phi_2^\dagger \phi_2^\dagger \mathbf{10}_j + h.c. . \quad (2.6)$$

Here, $\lambda_{L,E}$ denote coupling constants, and Λ_{cut} represents a cutoff scale greater than or comparable to the fake GUT scale [10]. The flavor indices are denoted by i and j . The higher-dimensional operator arises by integrating out fields heavier than the fake GUT scale (see Ref. [10] for details).

After the fake GUT symmetry breaking, the mass terms for the leptonic components take the form:

$$\mathcal{L}_{\text{mass}} = \bar{L}_{Hi} \mathcal{M}_{L,ij} \begin{pmatrix} L_{\bar{\mathbf{5}}} \\ L_H \end{pmatrix}_j + E_{Hi} \mathcal{M}_{E,ij} \begin{pmatrix} \bar{E}_{\mathbf{10}} \\ \bar{E}_H \end{pmatrix}_j + h.c. , \quad (2.7)$$

where $\mathcal{M}_{L,E}$ are the 3×6 mass matrices, given by:

$$\mathcal{M}_L = \begin{pmatrix} \lambda_L v_2 & m_L \end{pmatrix} , \quad \mathcal{M}_E = \begin{pmatrix} \frac{\lambda_E v_2^2}{\Lambda_{\text{cut}}} & m_E \end{pmatrix} . \quad (2.8)$$

Three leptons remain massless due to the rank conditions of these 3×6 matrices. As a result, the three generations of Weyl fermions of the SM are realized, although the SM leptons are not fully contained within $\bar{\mathbf{5}} \oplus \mathbf{10}$ unlike conventional SU(5) GUT models. On the other hand, all SM quarks are fully incorporated within $\bar{\mathbf{5}} \oplus \mathbf{10}$.

To explicitly show the emergence of SM leptons at low energy, let us ignore flavor mixing and focus on just one generation for simplicity. In this case, the mass eigenstates of the leptonic components are given by

$$\begin{pmatrix} L_M \\ \ell_{\text{SM}} \end{pmatrix} = \begin{pmatrix} \cos \theta_L & \sin \theta_L \\ -\sin \theta_L & \cos \theta_L \end{pmatrix} \begin{pmatrix} L_{\bar{\mathbf{5}}} \\ L_H \end{pmatrix} , \quad (2.9)$$

$$\begin{pmatrix} \bar{E}_M \\ \bar{e}_{\text{SM}} \end{pmatrix} = \begin{pmatrix} \cos \theta_E & \sin \theta_E \\ -\sin \theta_E & \cos \theta_E \end{pmatrix} \begin{pmatrix} \bar{E}_{\mathbf{10}} \\ \bar{E}_H \end{pmatrix} . \quad (2.10)$$

Here, ℓ_{SM} and \bar{e}_{SM} represent the massless eigenstates of the doublet and the singlet, respectively. Additionally, the leptonic mixing angles, $\theta_{L,E}$, are defined by

$$\tan \theta_L = \left| \frac{m_L}{\lambda_L v_2} \right| , \quad \tan \theta_E = \left| \frac{m_E \Lambda_{\text{cut}}}{\lambda_E v_2^2} \right| . \quad (2.11)$$

In this way, we obtain the SM leptons and quarks. Notably, the resultant fermions automatically fit into $\bar{\mathbf{5}} \oplus \mathbf{10}$ multiplets, despite not being embedded in a true GUT multiplet. We refer to this mechanism as the fake GUT, arising from the chiral structure of the SU(5) sector.

Note that in the limit where $m_{L,E} \rightarrow 0$, a global symmetry is enhanced, under which L_H and \bar{E}_H carry distinct charges. Thus, it is technically natural to assume that $m_{L,E}$ are small in the sense of

't Hooft's naturalness criterion [16]. In the small $m_{L,E}$ limit, SM leptons are fully contained in L_H and \bar{E}_H , while the heavy leptons, L_M and \bar{E}_M , remain massive. In this case, although the quarks and leptons in the SM originate from completely separate multiplets in the fake GUT, they appear to form $\bar{\mathbf{5}} \oplus \mathbf{10}$ multiplets at low energies. For future reference, we refer to this global symmetry as $U(1)_{LH}$ symmetry under which L_H and \bar{E}_H have charges, +1 and -1, respectively.

2.2 Origin of SM Higgs and Yukawa interactions

As discussed in the previous section, since the SM quarks and the SM leptons can have different UV origins, the SM Yukawa interactions are composed of various contributions. In this section, we show a concrete example of the origin of the SM Yukawa interactions. For that purpose, we introduce a scalar field, H_2 , which is in the $(\mathbf{1}, \mathbf{2})_{1/2}$ representation. We also introduce H_5 in the $(\mathbf{5}, \mathbf{1})_0$ representation, which decomposes as the triplet and doublet,

$$H_5 = H_C \oplus H_1 . \quad (2.12)$$

The two Higgs doublets, H_1 and H_2 , are mixed by the following interaction,

$$\mathcal{L}_{\text{mix}} = \mu_{\text{mix}} H_2 \phi_2 H_5^\dagger + h.c. , \quad (2.13)$$

where μ_{mix} is a mass parameter of $\mathcal{O}(v_2)$. After $SU(5) \times U(2)_H$ symmetry breaking, the Higgs doublets obtain the following effective mass terms,

$$\mathcal{L} = -m_1^2 |H_1|^2 - m_2^2 |H_2|^2 + (\mu_{\text{mix}} v_2 H_2 H_1^\dagger + h.c.) . \quad (2.14)$$

Here, m_1^2 and m_2^2 are mass parameters of $\mathcal{O}(v_2^2)$. The SM Higgs, h_{SM} , is given by an almost massless linear combination of H_1 and H_2 ,

$$h_{\text{SM}} = \sin \theta_h H_1 + \cos \theta_h H_2 . \quad (2.15)$$

To achieve the mass term of h_{SM} in $\mathcal{O}(100)$ GeV, we require fine-tuning similar to conventional GUT models.

By using H_5 and H_2 , the UV origins of the SM Yukawa interactions are given by,

$$\mathcal{L}_{YQ} = \frac{1}{4} y_{ij}^{(10)} \mathbf{10}_i \mathbf{10}_j H_5 - \sqrt{2} y_{ij}^{(5)} \mathbf{10}_i \bar{\mathbf{5}}_j H_5^\dagger + h.c. , \quad (2.16)$$

$$\mathcal{L}_{YL} = -y_{ij}^{(LE)} L_{Hi} \bar{E}_{Hj} H_2^\dagger + h.c. , \quad (2.17)$$

where i and j represent flavor indices. The parameters $y_{ij}^{(10)}$, $y_{ij}^{(5)}$ and $y_{ij}^{(LE)}$ are dimensionless couplings. The SM Yukawa couplings are obtained by substituting $H_5 \rightarrow \sin \theta_h h_{\text{SM}}$, $H_2 \rightarrow \cos \theta_h h_{\text{SM}}$ after diagonalizing the mass matrices in Eq. (2.8). For simplicity, we will omit the SM subscript when the SM fields are clear from context.

As we will discuss in Sec. 2.3, the lepton components in $\bar{\mathbf{5}} \oplus \mathbf{10}$ must be highly suppressed to avoid nucleon decay constraints, i.e., $|\theta_{L,E}| \ll 1$. In this case, the SM Yukawa interactions are given as,

$$\mathcal{L}_Y = -y_{ij}^{(u)} Q_i \bar{u}_j h - y_{ij}^{(d)} Q_i \bar{d}_j h^\dagger - y_{ij}^{(e)} \ell_i \bar{e}_j h^\dagger + h.c. , \quad (2.18)$$

where the SM Yukawa couplings are written by

$$\begin{aligned} y_{ij}^{(u)} &= \sin \theta_h y_{ij}^{(10)} , \\ y_{ij}^{(d)} &= \sin \theta_h y_{ij}^{(5)} , \\ y_{ij}^{(e)} &= \cos \theta_h y_{ij}^{(LE)} + \mathcal{O}(\theta_L \theta_E) \sin \theta_h y_{ji}^{(5)} . \end{aligned} \quad (2.19)$$

Here, $Q = (u, d)$, \bar{u} , \bar{d} are the doublet, the anti-up-type, and the anti-down-type quarks, while $\ell = (\nu, e)$, \bar{e} are the doublet and the anti-electron-type leptons with i, j as flavor indices. Since we assume $|\theta_{L,E}| \ll 10^{-4}$ to avoid too rapid proton decay, the $y^{(5)}$ contribution to $y_{ij}^{(e)}$ is negligible.

Finally, we describe the origin of the neutrino masses. In this model, we introduce three right-handed neutrinos, \bar{N}_a , $a = 1, 2, 3$. Following the seesaw mechanism [17–21], the origins of the Yukawa interactions to the right-handed neutrinos are given by,²

$$\mathcal{L}_\nu = -y_{ia}^{(LN)} L_{Hi} \bar{N}_a H_2 - \frac{1}{2} M_R y_{ab}^{(R)} \bar{N}_a \bar{N}_b + h.c. \quad (2.20)$$

Here, M_R represents the mass scale of the right-handed neutrinos, and the parameters $y_{ia}^{(5N)}$, $y_{ia}^{(LN)}$ and $y_{ab}^{(R)}$ are dimensionless coupling constants. Since we assume $|\theta_{L,E}| \ll 1$, the Yukawa interaction of the right-handed neutrinos is reduced to,

$$\mathcal{L}_\nu = -y_{ia}^{(D)} \ell_i \bar{N}_a h - \frac{1}{2} M_R y_{ab}^{(R)} \bar{N}_a \bar{N}_b + h.c. , \quad (2.21)$$

where the Yukawa couplings of the right-handed neutrino are expressed by

$$y_{ij}^{(D)} = \cos \theta_h y_{ij}^{(LN)} . \quad (2.22)$$

Below the right-handed neutrino mass scale, the Yukawa interaction in Eq. (2.21) induces effective dimension-five operators via the seesaw mechanism [17–21],

$$\mathcal{L}_\nu = -y_{ij}^{(S)} \frac{(\ell_i h)(\ell_j h)}{2M_R} + h.c. , \quad y_{ij}^{(S)} = -(y^{(D)}(y^{(R)})^{-1}(y^{(D)})^T)_{ij} . \quad (2.23)$$

With the VEV of the Higgs doublet, $\langle h \rangle = (0, v_{EW})^T$, the neutrinos ν_i obtain Majorana mass terms,

$$\mathcal{L}_{\text{mass}} = -\frac{1}{2} m_{ij}^{(\nu)} \nu_i \nu_j + h.c. , \quad m_{ij}^{(\nu)} = y_{ij}^{(S)} \frac{v_{EW}^2}{M_R} . \quad (2.24)$$

²In general, another Yukawa interaction, $y_{ia}^{(5N)} \bar{\mathbf{5}}_i \bar{N}_a H_5$, exists. In this paper, we do not consider this term.

Here, $v_{\text{EW}} \simeq 174 \text{ GeV}$, represents the electroweak scale.

Before concluding this section, we comment on $m_{L,E} \rightarrow 0$ limit in the presence of the neutrino interactions in Eq. (2.20). In this limit, the SM charged leptons reside entirely in L_H 's, and hence, the presence of neutrino mass requires $y^{(LN)} \neq 0$. For the seesaw mechanism to work, we assume $M_R \neq 0$, which explicitly breaks the $U(1)_{LH}$ symmetry down to Z_2 symmetry. Despite the breaking of $U(1)_{LH}$ symmetry, proton stability is maintained for $m_{L,E} = 0$ due to the remaining Z_2 symmetry.

2.3 Nucleon decay

Nucleons can decay for $m_{L,E} \neq 0$ through the exchange of heavy SU(5) gauge bosons, similar to the conventional GUT models.³ However, as discussed in Sec. 2.1, since the origins of the SM quarks and the SM leptons are different, the interaction related to nucleon decay is suppressed by the leptonic mixing angles, $|\sin \theta_{L,E}|^2$, as shown in Fig. 1. Let us evaluate the proton lifetime in the simple case

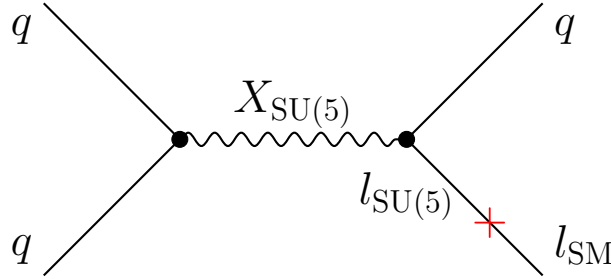


Figure 1: Baryon and lepton number-violating interaction through the exchange of a heavy SU(5) gauge boson, X . The red cross mark represents the mixing of $L_{\bar{5}}$ (\bar{E}_{10}) with l_{SM} (\bar{e}_{SM}).

where only the first generation leptons have mixing angle $\theta_{L,E}$ in Eqs. (2.9) and (2.10). In this case, the partial proton lifetime for the $p \rightarrow \pi^0 e^+$ mode is given by

$$\tau(p \rightarrow \pi^0 e^+) \simeq \frac{5 \times 10^{26} \text{ years}}{\sin^2 \theta_E + 0.2 \sin^2 \theta_L} \left(\frac{M_X / g_5}{10^{14} \text{ GeV}} \right)^4. \quad (2.25)$$

Here, M_X and g_5 denote the mass of the heavy SU(5) gauge boson and the gauge coupling of SU(5). This lifetime is consistent with the current experimental limit, $\tau(p \rightarrow \pi^0 e^+) > 2.4 \times 10^{34} \text{ years}$ [5], for small mixing angles, $|\sin \theta_{E,L}| \lesssim 10^{-4}$ even for $M_X = 10^{14} \text{ GeV}$. Therefore, the result in Eq. (2.25) indicates that small mixing angles for both $L_{\bar{5}}$ and \bar{E}_{10} with SM leptons are necessary to satisfy the experimental constraints.⁴

In general, the lepton mass matrices in Eq. (2.8) are flavor-dependent. In this case, the flavor composition of the leptonic components $L_{\bar{5},i}$ and $\bar{E}_{10,i}$ in the SU(5) sector does not necessarily coincide with the generations of the SM leptons in their mass eigenstates. Consequently, the predictions

³In Ref. [10], we found that there is an upper limit on the heavy SU(5) gauge boson mass, M_X , of $M_X^{\text{upper}} \simeq 10^{14.4} \text{ GeV}$. This upper limit is derived by requiring a consistent matching of the gauge couplings between the fake GUT and the SM at the fake GUT scale, $\mu_R = M_X$.

⁴Nucleons can also decay through the exchange of the colored Higgs bosons. However, this process has been shown to be suppressed [10].

of the nucleon decay rates and the branching fractions are different from those in the conventional GUT (see Ref. [10] for details). In Sec. 4, we will discuss predictions for nucleon decay rates and branching fractions within the FN mechanism.

3 Froggatt-Nielsen Mechanism

3.1 Explanation of Froggatt-Nielsen mechanism

The FN mechanism is one of the most successful models for explaining the hierarchy of the charged fermion masses and the quark mixing angles [15]. In this mechanism, a new $U(1)_{\text{FN}}$ flavor symmetry, $U(1)_{\text{FN}}$, and a new complex scalar field Φ are introduced. Under the $U(1)_{\text{FN}}$ symmetry, quarks and leptons of different generations have distinct $U(1)_{\text{FN}}$ charges, and Φ has an FN charge of -1 . The $U(1)_{\text{FN}}$ is spontaneously broken when Φ acquires a VEV, $\langle \Phi \rangle$.⁵

Let us first consider the SM Yukawa interactions. Due to the $U(1)_{\text{FN}}$ symmetry, the Yukawa interactions are modified as

$$\mathcal{L}_Y = \kappa_{ij} \left(\frac{\Phi^{(\dagger)}}{M_*} \right)^{|f_{\psi,i} + f_{\chi,j}|} \psi_i \chi_j h_{\text{SM}}^{(\dagger)} + h.c. \quad (3.1)$$

Here, M_* denotes a cutoff scale, and κ represents 3×3 complex matrices of $\mathcal{O}(1)$. The fields ψ_i and χ_i collectively denote Q_i , L_i , and \bar{u}_i , \bar{d}_i , \bar{e}_i (see Eq. (2.18)). The parameters $f_{\psi,i}$ and $f_{\chi,i}$ denote the FN charges of the quarks and leptons, and we assume that the Higgs boson does not carry any FN charge. Due to the locality of the effective field theory, \mathcal{L}_Y includes only positive integer powers of Φ when $f_{\psi,i} + f_{\chi,j} > 0$, and positive integer powers of Φ^\dagger when $f_{\psi,i} + f_{\chi,j} < 0$.

Once Φ acquires a VEV, the $U(1)_{\text{FN}}$ -symmetric terms in Eq. (3.1) give rise to the SM Yukawa interactions,

$$y_{ij}^{(u)} = \kappa_{ij}^{(u)} \epsilon^{q_{ij}^{(u)}}, \quad y_{ij}^{(d)} = \kappa_{ij}^{(d)} \epsilon^{q_{ij}^{(d)}}, \quad y_{ij}^{(e)} = \kappa_{ij}^{(e)} \epsilon^{q_{ij}^{(e)}}. \quad (3.2)$$

Here, summation over i, j is not implied in Eq. (3.2).⁶ The FN breaking parameter, ϵ , and the exponents q_{ij} are defined as

$$\epsilon \equiv \frac{\langle \Phi \rangle}{M_*} = \frac{\langle \Phi^\dagger \rangle}{M_*}, \quad (3.3)$$

$$q_{ij}^{(u)} = |f_{Q,i} + f_{\bar{u},j}|, \quad q_{ij}^{(d)} = |f_{Q,i} + f_{\bar{d},j}|, \quad q_{ij}^{(e)} = |f_{L,i} + f_{\bar{e},j}|. \quad (3.4)$$

Here, we have taken $\epsilon > 0$ without loss of generality. Since we assume $\epsilon = \mathcal{O}(0.1)$, the above couplings are more suppressed for larger values of q_{ij} , which generates non-trivial hierarchies of the Yukawa couplings even for κ 's of $\mathcal{O}(1)$.

⁵To avoid a Goldstone boson associated with spontaneous $U(1)_{\text{FN}}$ breaking, we assume the presence of explicit $U(1)_{\text{FN}}$ breaking of a magnitude that does not spoil the FN mechanism. Alternatively, we may consider a discrete Z_N symmetry with a large order N instead of $U(1)_{\text{FN}}$.

⁶When all $f_i + f_j$ have the same sign, the term $\kappa_{ij} \epsilon^{f_i + f_j}$ can be expressed as a matrix multiplication: $\kappa_{ij} \epsilon^{f_i + f_j} = (\epsilon^f \cdot \kappa \cdot \epsilon^f)_{ij}$, where $\epsilon_{ij}^f = \epsilon^{f_i} \delta_{ij}$.

The FN mechanism also affects the masses and mixing structure of neutrinos. The Yukawa coupling constants of the neutrino sector are given by

$$y_{ia}^{(D)} = \kappa_{ia}^{(D)} \epsilon^{q_{ia}^{(D)}} , \quad y_{ab}^{(R)} = \kappa_{ab}^{(R)} \epsilon^{q_{ab}^{(R)}} , \quad (3.5)$$

$$q_{ia}^{(D)} = |f_{L,i} + f_{\bar{N},a}| , \quad q_{ab}^{(R)} = |f_{\bar{N},a} + f_{\bar{N},b}| . \quad (3.6)$$

Here, $\kappa^{(D)}$ is a complex 3×3 matrix, while $\kappa^{(R)}$ is a complex 3×3 symmetric matrix. As before, summation over i, a, b is not implied in Eq. (3.5).

In the conventional SU(5) GUT, the FN charges of the quarks and leptons satisfy the relations,

$$f_{Q,i} = f_{\bar{u},i} = f_{\bar{e},i} = f_{\mathbf{10},i} , \quad f_{\bar{d},i} = f_{L,i} = f_{\bar{\mathbf{5}},i} , \quad (3.7)$$

since they are embedded within $\mathbf{10}$ and $\bar{\mathbf{5}}$ representations. Due to the $U(1)_{\text{FN}}$ symmetry, the Yukawa interactions in the GUT (similar to those described by Eq. (2.16)) are modified in a manner analogous to Eq. (3.1). The FN charges of the right-handed neutrinos, however, can be chosen independently. In the minimal supersymmetric SU(5) GUT model, for example, the following charge assignments were proposed in Ref. [22],

$$\epsilon \sim 0.06 , \quad f_{\mathbf{10}} = (2, 1, 0) , \quad f_{\bar{\mathbf{5}}} = (a + 1, a, a) , \quad f_{\bar{N}} = (d, c, b) , \quad (3.8)$$

where $a = 0$ or 1 and $0 \leq b \leq c \leq d$ (see also Ref. [23]).

In the $SU(5) \times U(2)_H$ fake GUT model, since the quarks originate from the SU(5) multiplets, the effective Yukawa couplings in the quark sector are determined by the FN charges of $\bar{\mathbf{5}}_i$ and $\mathbf{10}_i$, similar to the conventional GUT. The Yukawa interactions for charged leptons, on the other hand, have two UV origins as shown in Eq. (2.19). However, as mentioned earlier, lepton mixing angles in Eqs. (2.9) and (2.10) are highly suppressed to avoid the constraints from the proton decay. Accordingly, the SM leptons almost entirely originate from L_H and \bar{E}_H and the SM lepton Yukawa coupling is effectively given by $y^{(LE)}$, regardless of the details of the lepton mixing angles, $\theta_{L,E}$. Accordingly, the flavor structure of the charged lepton Yukawa coupling is determined by the FN charges of L_{Hi} and \bar{E}_{Hi} . Besides, since the right-handed neutrino Yukawa coupling is given by Eq. (2.20), the flavor structure of the neutrino Yukawa couplings is determined by the FN charges of L_{Hi} and \bar{N}_a .

Altogether, the relevant FN charges in the $SU(5) \times U(2)_H$ fake GUT model are

$$f_{\mathbf{10}} , \quad f_{\bar{\mathbf{5}}} , \quad f_{L_H} , \quad f_{\bar{E}_H} , \quad f_{\bar{N}} . \quad (3.9)$$

Effective Yukawa couplings are obtained by using these FN charges,

$$y_{ij}^{(10,5,LE,LN,R)} = \kappa_{ij}^{(10,5,LE,LN,R)} \epsilon^{q_{ij}^{(10,5,LE,LN,R)}} , \quad (3.10)$$

$$q_{ij}^{(10)} = |f_{\mathbf{10},i} + f_{\mathbf{10},j}| , \quad q_{ij}^{(5)} = |f_{\mathbf{10},i} + f_{\bar{\mathbf{5}},j}| , \quad (3.11)$$

$$q_{ij}^{(LE)} = |f_{L_H,i} + f_{\bar{E}_H,j}| , \quad q_{ij}^{(LN)} = |f_{L_H,i} + f_{\bar{N},j}| , \quad q_{ij}^{(R)} = |f_{\bar{N},i} + f_{\bar{N},j}| . \quad (3.12)$$

Note that the FN charge assignment of \bar{L}_{Hi} and E_{Hi} do not affect the flavor structure of the leptons as long as $|\theta_{L,E}| \ll 1$. In the next section, we show examples of the FN charge assignment.

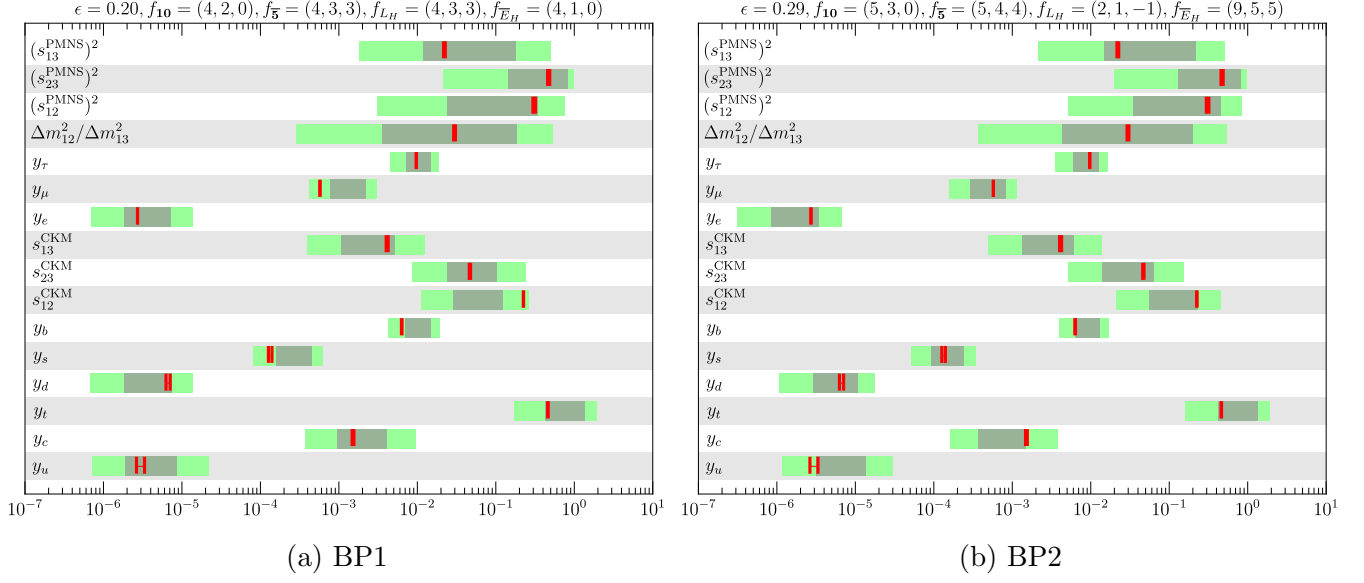


Figure 2: The prior distributions for the SM parameters from $\mathcal{O}(1)$ distributions of κ 's with the FN charge assignments in Eqs. (3.13) and (3.14). The red bars represent the values of the running parameters estimated within the $\overline{\text{MS}}$ scheme at $\mu_R = 10^{14}$ GeV. The observed values are within the ranges of the posterior distributions.

3.2 Benchmark FN charge assignment in the $\text{SU}(5) \times \text{U}(2)_H$ model

In our analysis, we compare the SM parameters predicted by the FN mechanism with those evaluated in the $\overline{\text{MS}}$ scheme at the renormalization scale $\mu_R = 10^{14}$ GeV. We use the PDG averages of the SM particle masses [24] as input parameters, and relevant renormalization group equations (RGEs) in the $\overline{\text{MS}}$ [25]. We estimate the Yukawa couplings of the light quarks, by using the QCD four-loop RGEs and three-loop decoupling effects from heavy quarks [26]. Note that the discussion is not highly sensitive to the choice of the renormalization scale, as long as it is significantly higher than the electroweak scale. This is because the dominant renormalization group effects stem from QCD interactions below the electroweak scale. For this reason, we also neglect the running effects between μ_R and M_* .

For the neutrino mass parameters, we do not account for the renormalization group effects, since the relative sizes of the FN breaking scale and M_R are not fixed in this work. Moreover, the renormalization group effects in the SM interaction have a negligible impact on the neutrino mass ratio and mixing angles, which are utilized in the following analysis.

In this paper, we take two benchmark points for the FN charge assignments of the fake GUT multiplets,

$$\text{BP1: } \epsilon = 0.20, \quad f_{10} = (4, 2, 0), \quad f_{\bar{5}} = (4, 3, 3), \quad f_{L_H} = (4, 3, 3), \quad f_{\bar{E}_H} = (4, 1, 0), \quad (3.13)$$

$$\text{BP2: } \epsilon = 0.29, \quad f_{10} = (5, 3, 0), \quad f_{\bar{5}} = (5, 4, 4), \quad f_{L_H} = (2, 1, -1), \quad f_{\bar{E}_H} = (9, 5, 5). \quad (3.14)$$

Here, we set all $f_{\bar{N},a} = 0$ ($a = 1, 2, 3$) and $\sin \theta_h = \cos \theta_h = 1/\sqrt{2}$ for simplicity. Additionally, we

assume H_5 and H_2 do not have any FN charges.

In Fig. 2, we present the distributions of the predicted parameters for these FN charge assignments with random $\mathcal{O}(1)$ coefficients κ 's. We assume the normal neutrino mass ordering, i.e., ($m_1 < m_2 < m_3$). The dark green and light green bands represent the 1σ and 2σ percentiles, respectively. The red bars indicate the values of the running parameters which are estimated in the $\overline{\text{MS}}$ scheme at $\mu_R = 10^{14}$ GeV. From this figure, we find that the observed physical parameters are within typical ranges of the predictions of the FN mechanism with the above FN charge assignments.

In the above analysis, we adopt the following distributions for the $\mathcal{O}(1)$ coefficients $\kappa^{(10,5,LE,LN,R)}$ in Eq. (3.10). For the Dirac-type couplings $\kappa_{ij}^{(10,5,LE,LN)}$, we use the following distributions,

$$\text{Re } \kappa_{ij}^{(10,5,LE,LN)} = \frac{1}{\sqrt{2}} \mathcal{N}(0, 1) , \quad \text{Im } \kappa_{ij}^{(10,5,LE,LN)} = \frac{1}{\sqrt{2}} \mathcal{N}(0, 1) . \quad (3.15)$$

Here, $\mathcal{N}(0, 1)$ denotes a random number drawn from a normal distribution with a mean of 0 and a standard deviation of 1. Similarly, for the Majorana-type couplings $\kappa_{ij}^{(R)}$, we assume the following distributions,

$$\begin{aligned} \text{Re } \kappa_{aa}^{(R)} &= \frac{1}{\sqrt{2}} \mathcal{N}(0, 1) , \quad \text{Im } \kappa_{aa}^{(R)} = \frac{1}{\sqrt{2}} \mathcal{N}(0, 1) , \\ \text{Re } \kappa_{ab}^{(R)} &= \frac{1}{2} \mathcal{N}(0, 1) , \quad \text{Im } \kappa_{ab}^{(R)} = \frac{1}{2} \mathcal{N}(0, 1) , \quad (a > b) . \end{aligned} \quad (3.16)$$

Note that we assume the variance of the off-diagonal elements is smaller than that of the diagonal elements by a factor of $\sqrt{2}$, which makes the distributions flavor symmetric.

4 Nucleon Decay with U(1) Flavor Symmetry

As mentioned earlier, the generation of the leptonic components in $L_{\bar{5},i}$ and $\bar{E}_{10,i}$ within the SU(5) sector does not align with that of the SM leptons in the mass eigenstates. In this section, we discuss how the FN charge assignments affect the flavor dependence of the leptonic components in $L_{\bar{5},i}$ and $\bar{E}_{10,i}$, which provides striking effects on the nucleon decay rates and the branching fractions.

4.1 Flavor effects on lepton mixing angles

Let us discuss the effects of the FN mechanism on the lepton mixing terms in Eq. (2.6). Under the FN mechanism, they are modified as,

$$\begin{aligned} \mathcal{L} &= \bar{m}_L \kappa_{ij}^{(m_L)} \epsilon^{f_{\bar{L}_H,i} + f_{L_H,j}} \bar{L}_{Hi} L_{Hj} + \kappa_{ij}^{(\lambda_L)} \epsilon^{f_{\bar{L}_H,i} + f_{\bar{5},j}} \bar{L}_{Hi} \phi_2 \bar{5}_j \\ &+ \bar{m}_E \kappa_{ij}^{(m_E)} \epsilon^{f_{E_H,i} + f_{E_H,j}} E_{Hi} \bar{E}_{Hj} + \frac{\kappa_{ij}^{(\lambda_E)}}{\Lambda_{\text{cut}}} \epsilon^{f_{E_H,i} + f_{10,j}} E_{Hi} \phi_2^\dagger \phi_2^\dagger \mathbf{10}_j + h.c. \end{aligned} \quad (4.1)$$

Here, κ 's are dimensionless $\mathcal{O}(1)$ coefficients that follow the Gaussian distribution for Dirac-type couplings described in the previous section. The parameters \bar{m}_L and \bar{m}_E are dimensionful constants.

We assume ϕ_2 does not have the FN charge. We also focus on the case where each sums of the FN charges in Eq. (4.1) are larger than or equal to 0. In subsequent calculations, we choose the values for \overline{m}_L , \overline{m}_E and Λ_{cut} to achieve the tiny lepton mixing angles in Eqs. (2.9) and (2.10). The relationships between the coefficients of Eqs. (2.6) and (4.1) are given by

$$\begin{aligned} m_{L,ij} &= \overline{m}_L \kappa_{ij}^{(m_L)} \epsilon^{f_{\overline{L}_H, i} + f_{L_H, j}} , & \lambda_{L,ij} &= \kappa_{ij}^{(\lambda_L)} \epsilon^{f_{\overline{L}_H, i} + f_{\overline{5}, j}} , \\ m_{E,ij} &= \overline{m}_E \kappa_{ij}^{(m_E)} \epsilon^{f_{E_H, i} + f_{\overline{E}_H, j}} , & \lambda_{E,ij} &= \kappa_{ij}^{(\lambda_E)} \epsilon^{f_{E_H, i} + f_{10, j}} . \end{aligned} \quad (4.2)$$

Note that the summation over the flavor indices $i, j = 1, 2, 3$ is not taken.

Let us consider the mass terms of the doublet leptons in Eq. (2.7),

$$\begin{aligned} \mathcal{L}_{\text{mass}} &= \overline{L}_{Hi} \begin{pmatrix} \lambda_{L,ij} v_2 & m_{L,ik} \end{pmatrix} \begin{pmatrix} L_{\overline{5},j} \\ L_{Hk} \end{pmatrix} \\ &= (\overline{L}_{Hi} \lambda_{L,ij} v_2) (L_{\overline{5},j} + v_2^{-1} (\lambda_L^{-1})_{jn} m_{L,nk} L_{Hk}) . \end{aligned} \quad (4.3)$$

From this expression, the heavy leptons L_{Mi} and the SM leptons $\ell_{\text{SM},i}$ are given by,

$$L_{Mi} \simeq L_{\overline{5},i} + v_2^{-1} (\lambda_L^{-1})_{ik} m_{L,kj} L_{Hj} , \quad (4.4)$$

$$\ell_{\text{SM},i} \simeq L_{Hi} - v_2^{-1} (\lambda_L^{-1})_{ik} m_{L,kj} L_{\overline{5},j} . \quad (4.5)$$

Thus, for small lepton mixing angles θ_L , we find that the $L_{\overline{5}}$'s include the SM lepton contents as,

$$L_{\overline{5},i} \simeq L_{Mi} - v_2^{-1} (\lambda_L^{-1})_{ik} m_{L,kj} \ell_{\text{SM},j} . \quad (4.6)$$

Furthermore, for the case where each sum of the FN charges in Eq. (4.1) is larger than or equal to 0, as we are considering, $\lambda_L^{-1} m_L$ does not depend on the FN charge of \overline{L}_H . Let us see this explicitly. In this case, λ_L and m_L can be expressed as products of matrices,

$$\lambda_L = \epsilon^{f_{\overline{L}_H}} \kappa^{(\lambda_L)} \epsilon^{f_{\overline{5}}} , \quad m_L = \overline{m}_L \epsilon^{f_{\overline{L}_H}} \kappa^{(m_L)} \epsilon^{f_{L_H}} , \quad (4.7)$$

where $\epsilon_{ij}^f = \epsilon^f \delta_{ij}$. Therefore, $\lambda_L^{-1} m_L$ is given as

$$(\lambda_L)^{-1} m_L = \overline{m}_L (\epsilon^{f_{\overline{5}}})^{-1} (\kappa^{(\lambda_L)})^{-1} (\epsilon^{f_{\overline{L}_H}})^{-1} \epsilon^{f_{\overline{L}_H}} \kappa^{(m_L)} \epsilon^{f_{L_H}} = \overline{m}_L (\epsilon^{f_{\overline{5}}})^{-1} (\kappa^{(\lambda_L)})^{-1} \kappa^{(m_L)} \epsilon^{f_{L_H}} . \quad (4.8)$$

This shows that the FN charge matrix of \overline{L}_H cancels out in $\lambda_L^{-1} m_L$. As a result, the SM lepton components in the $L_{\overline{5}}$ are independent of the FN charges of \overline{L}_{Hi} , since they are evaluated as

$$(\theta_L)_{ij} = v_2^{-1} (\lambda_L^{-1})_{ik} m_{L,kj} \sim \overline{\theta}_L \times \epsilon^{-f_{\overline{5},i} + f_{L_H,j}} . \quad (4.9)$$

The same procedure applies to the case of the singlet leptons \overline{E}_H ,

$$(\theta_E)_{ij} = v_2^{-2} \Lambda_{\text{cut}} (\lambda_E^{-1})_{ik} m_{E,kj} \sim \overline{\theta}_E \times \epsilon^{-f_{10,i} + f_{\overline{E}_H,j}} . \quad (4.10)$$

For later purpose, we have defined

$$\bar{\theta}_L = \frac{\bar{m}_L}{v_2} , \quad \bar{\theta}_E = \frac{\bar{m}_E \Lambda_{\text{cut}}}{v_2^2} . \quad (4.11)$$

A notable feature of the FN mechanism in the fake GUT is that SM lepton contents within the SU(5) multiplets in Eq. (4.9) tend to be more suppressed for the lower generations. This is because the L_H and \bar{E}_H of the lower generations has larger FN charges, and the generations of these vector-like leptons correspond to those of the SM leptons. Therefore, nucleons are more likely to decay into the SM leptons of the higher generations.

As discussed in Sec. 2.3, the lepton mixing angles $\theta_{L,E}$ must be constrained to be below $\mathcal{O}(10^{-4})$ to avoid violating nucleon lifetime constraints. For the two benchmark points, BP1 and BP2, this requires the $U(1)_{LH}$ breaking parameters to be on the order of $\bar{m}_{L,E} \simeq 10^{8-9} \text{ GeV}$, given that $\Lambda_{\text{cut}} \gtrsim v_2$. This scale is reasonably close to the right-handed neutrino mass scale M_R , which is relevant for the seesaw mechanism under the assumptions for these benchmark points. Although we do not explore this further in the present work, this observation suggests that the origin of the $U(1)_{LH}$ symmetry-breaking parameters \bar{m}_L , \bar{m}_E , and M_R may have a common origin in a unified sector.

4.2 Flavorful nucleon decay

Now, let us discuss the predictions of nucleon decay. For given values of κ , we first transform the random flavor basis of SU(5) multiplets to a basis where the up-type Yukawa matrix is diagonal, and the down-type Yukawa matrix is given by the diagonal matrix multiplied by the CKM matrix, as described in Ref. [27]. We also extract the SM lepton components, which correspond to the massless eigenstates of the lepton mass matrices in Eq. (2.8)). Subsequently, we transform the SM leptons to their mass basis. In this way, we obtain the lepton components in the mass basis of the SU(5) multiplets in the down-type CKM basis as

$$L_{\bar{\mathbf{5}},i} \supset (\theta_L)_{ij} \ell_{\text{SM},j} , \quad \bar{E}_{\mathbf{10},i} \supset (\theta_E)_{ij} \bar{e}_{\text{SM},j} , \quad (4.12)$$

for each realization. Note that θ_L and θ_E are 3×3 matrices, and do not depend on either f_{LH} 's or f_{EH} 's.

Once we obtain these matrices, we can calculate the nucleon decay rate using the following operators,

$$\mathcal{O}_{ijkl}^{(1)} = \epsilon_{abc} \left(\bar{u}_i^{\dagger a} \bar{d}_j^{\dagger b} \right) (Q_k^c L_{\bar{\mathbf{5}},l}) , \quad \mathcal{O}_{ijkl}^{(2)} = \epsilon_{abc} (Q_i^a Q_j^b) \left(\bar{u}_k^{\dagger c} \bar{E}_{\mathbf{10},l}^{\dagger} \right) , \quad (4.13)$$

which are generated by the heavy SU(5) gauge bosons (see Fig. 1). The Wilson coefficients for these operator are given by

$$C_{(1)}^{ijkl} = -\frac{g_5^2}{M_X^2} e^{i\varphi_i} \delta^{ik} \delta^{jl} , \quad C_{(2)}^{ijkl} = -\frac{g_5^2}{M_X^2} e^{i\varphi_k} \delta^{ik} \delta^{jl} . \quad (4.14)$$

Here, the phases, φ_i , satisfy $\sum_i \varphi_i = 0$, and arise from the basis transformation explained earlier. These operators are given at the fake GUT scale. In order to get low-energy observable predictions, we solve the RGE equations of these Wilson coefficients following Refs. [28, 29].

In our analysis, we utilize matrix elements for proton decay estimated by the QCD lattice calculation in Ref. [30]. For η meson modes, we use the results in Ref. [31]. Additionally, we obtain the neutron matrix elements for baryon number-violating neutron decays through the SU(2) isospin symmetry of QCD matrix elements. Therefore, the neutron decay rate into a pion has correlation with the proton decay rate into a pion as follows,

$$\Gamma(n \rightarrow \pi^- \ell_i^+) = 2 \Gamma(p \rightarrow \pi^0 \ell_i^+) , \quad (4.15)$$

$$\Gamma(n \rightarrow \pi^0 \bar{\nu}) = \frac{1}{2} \Gamma(p \rightarrow \pi^+ \bar{\nu}) . \quad (4.16)$$

Moreover, while the proton can decay into modes including a charged kaon, the neutron cannot decay into such modes within this model. This follows from the following Gell-Mann-Nishijima formula, which describes the relationship between various quantum numbers of a particle:

$$Q = I_3 + \frac{1}{2} (B + S) , \quad (4.17)$$

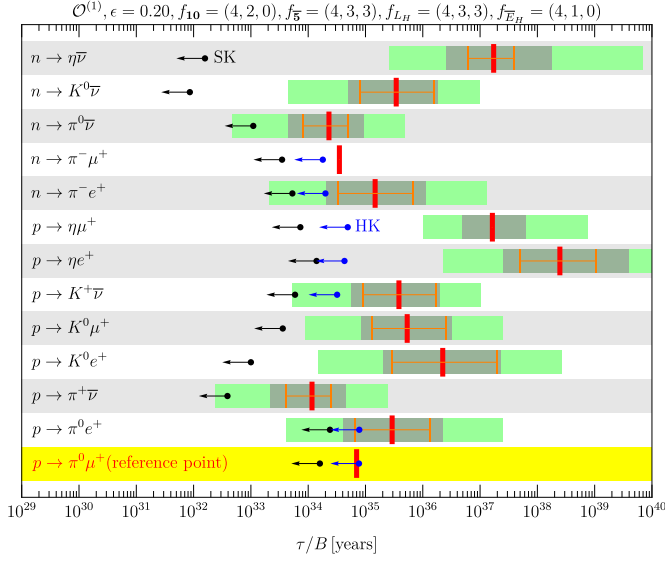
where Q, I_3, B and S denote the electric charge, the third component of the SU(2) isospin, the baryon number and the strangeness of a particle, respectively. Since electric charge is conserved, the decay $n \rightarrow K^- \ell_i^+$ is forbidden [32, 33].

To obtain predictions for nucleon decays, we follow the Monte-Carlo procedure outlined below. For given sets of the FN charges and the FN breaking parameter ϵ in Eqs. (3.13) and (3.14), we first generate all the κ values by sampling from Gaussian distributions in Eqs. (3.15) and (3.16). We obtain posterior distributions of κ 's which take into the observed parameters (the masses and mixing angles of the SM quarks and SM leptons) in Fig. 2. From those posterior distributions, we predict the nucleon decay rates for each decay mode. We also incorporate uncertainties from the QCD matrix elements in the predictions.

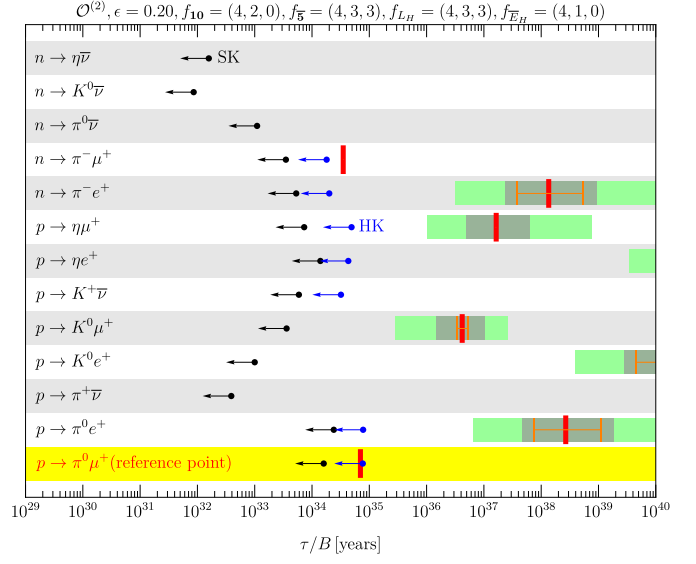
4.3 Results

The contributions of $\mathcal{O}^{(1)}$ and $\mathcal{O}^{(2)}$ to the nucleon decay amplitudes are suppressed by $\bar{\theta}_L$ and $\bar{\theta}_E$, respectively. We therefore treat these contributions independently. As we will demonstrate, $p \rightarrow \pi^0 \mu^+$ mode is one of the most promising discovery channels in the present model, and hence we choose this decay mode as a reference point. In the following analysis, we fix $M_X = 10^{14}$ GeV, and adjust either $\bar{\theta}_L$ or $\bar{\theta}_E$ such that the lifetime of the $p \rightarrow \pi^0 \mu^+$ mode is 7.0×10^{34} years for each realization of κ values. The distributions of other decay modes are provided relative to this fixed lifetime for the $p \rightarrow \pi^0 \mu^+$ mode.

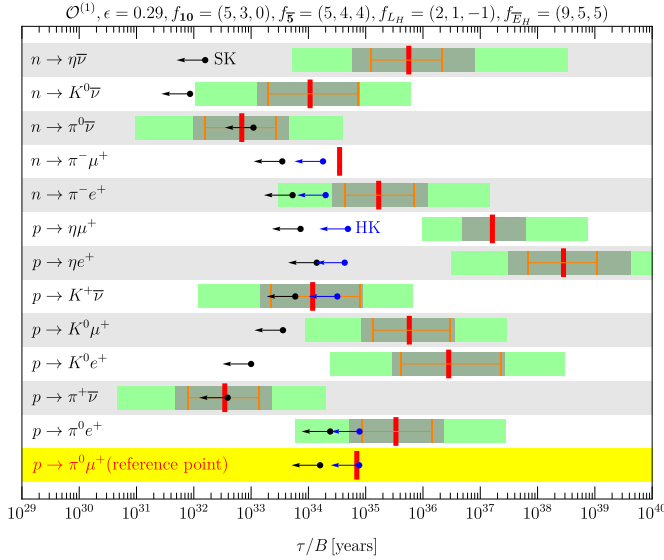
In Fig. 3, we present the percentile ranges of the posterior distributions for the predicted nucleon lifetimes across various decay modes for the FN charge assignments of BP1 and BP2. In Figs. 3a and



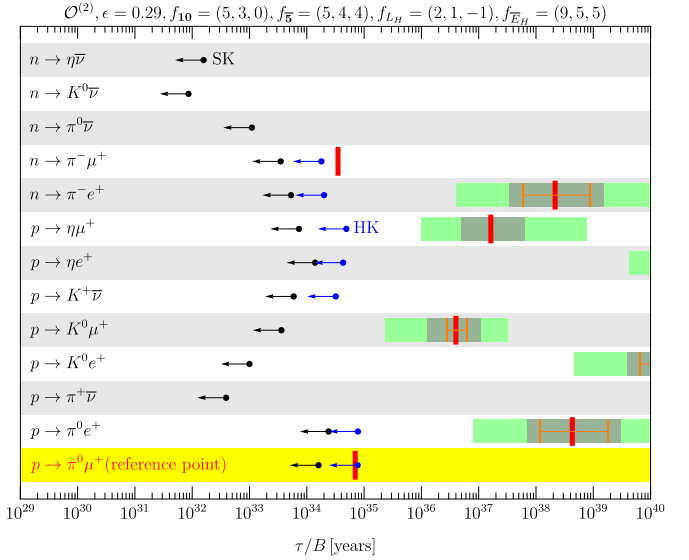
(a) Contribution of $\mathcal{O}^{(1)}$ (or $\bar{\theta}_E = 0$) for BP1.



(b) Contribution of $\mathcal{O}^{(2)}$ (or $\bar{\theta}_L = 0$) for BP1.



(c) Contribution of $\mathcal{O}^{(1)}$ (or $\bar{\theta}_E = 0$) for BP2.



(d) Contribution of $\mathcal{O}^{(2)}$ (or $\bar{\theta}_L = 0$) for BP2.

Figure 3: The nucleon lifetimes for various decay modes in benchmark points BP1 and BP2. Figures (a) and (b) show the nucleon decay originating from the operators $\mathcal{O}^{(1)}$ and $\mathcal{O}^{(2)}$ in Eq. (4.13) for BP1, respectively. Figures (c) and (d) illustrate the same for BP2. We set $M_X = 10^{14}$ GeV and adjust $\bar{\theta}_L$ and $\bar{\theta}_E$ to achieve a reference nucleon lifetime for the $p \rightarrow \pi^0 \mu^+$ decay mode of 7.0×10^{34} years. The dark green and light green bands represent the 1σ and 2σ percentile ranges of the lifetime distributions, with median values indicated by red bars. Orange bars depict the 1σ percentile range excluding uncertainties in QCD matrix elements. Current constraints from SK are shown with black arrows [5, 34–38], and future projections for HK are indicated with blue arrows [6].

3b (Figs. 3c and 3d), we illustrate the nucleon lifetimes arising from the nucleon decay operators $\mathcal{O}^{(1)}$ ($\mathcal{O}^{(2)}$) in Eq. (4.13). For decay modes involving $\bar{\nu}$, we sum over the contributions from all neutrino flavors. The dark green and light green bands represent the 1σ and 2σ percentile ranges of the distributions, respectively, with red bars indicating the medians. The orange bars represent the 1σ percentile range arising from uncertainties in the $\mathcal{O}(1)$ coefficients, κ , while excluding uncertainties in the QCD matrix elements. This uncertainty typically affects the predicted lifetime by a factor of $\mathcal{O}(10)$. Note that the ratio $\tau(n \rightarrow \pi^- \mu^+)/\tau(p \rightarrow \pi^0 \mu^+)$ is free from uncertainty due to the SU(2) isospin symmetry in Eq. (4.15). The uncertainty in the ratio $\tau(p \rightarrow \eta \mu^+)/\tau(p \rightarrow \pi^0 \mu^+)$ is primarily driven by the uncertainty in the QCD matrix element, with no contribution from the κ 's since these decays are caused by the common effective operators at the QCD scale. Black and blue arrows indicate current constraints from SK [5, 34–38] and the future projections for HK [6].

These figures highlight a clear contrast with the minimal SU(5) GUT. In the minimal SU(5) GUT, the dominant decay mode is $p \rightarrow \pi^0 e^+$, with other lepton flavor modes being significantly suppressed. In contrast, within the fake GUT, the generations of quarks and leptons are not aligned, allowing for a broader spectrum of decay modes. Specifically, under the FN mechanism, each SU(5) multiplet includes substantial contributions from the second and third generations of SM leptons. Consequently, nucleon decays into μ^+ and $\bar{\nu}_{\mu,\tau}$ are more likely. The figures demonstrate that the $p \rightarrow \pi^0 \mu^+$ mode emerges as a leading discovery channel. This distinctive feature of the FN mechanism within the fake GUT is clearly depicted in the figures for both BP1 and BP2. Additionally, it should be noted that the FN mechanism does not alter nucleon decay modes mediated by GUT gauge boson exchange in the minimal GUT. Therefore, detecting various lepton flavor modes would be highly effective for probing the fake GUT.

The notable difference between Figs. 3a and 3b arises because $\mathcal{O}^{(1)}$ includes a doublet lepton, while $\mathcal{O}^{(2)}$ contains a singlet lepton. This difference results in the absence of neutrino modes in Fig. 3b, which are present in Fig. 3a. A similar pattern is observed between Fig. 3c and Fig. 3d. In contrast, in the minimal SU(5) GUT, the contribution from $\mathcal{O}^{(2)}$ to $\Gamma(p \rightarrow \pi^0 e^+)$ is approximately four times larger than that from $\mathcal{O}^{(1)}$. Consequently, the search for neutrino decay modes serves as an essential probe for distinguishing the fake GUT.

As we can see in Eq. (4.9), the difference in $\tau(p \rightarrow \pi^0 e^+)/\tau(p \rightarrow \pi^0 \mu^+)$ between Figs. 3a and 3b primarily stems from the variations in $f_{LH,2} - f_{LH,1}$ and $f_{\bar{E}H,2} - f_{\bar{E}H,1}$. The greater this charge difference, the larger the ratio $\tau(p \rightarrow \pi^0 e^+)/\tau(p \rightarrow \pi^0 \mu^+)$ becomes. This behavior also applies to the baryon-number violating neutron decay. This result contrasts with conventional GUT predictions, where the ratio is $\tau(p \rightarrow \pi^0 e^+)/\tau(p \rightarrow \pi^0 \mu^+) = \mathcal{O}(10^{-(2-3)})$.

The figures illustrate that the predicted branching fractions are influenced by the FN charges. For example, decays into neutrino modes in Fig. 3c proceed more rapidly than those in Fig. 3a. This difference arises from the ratios of the lepton mixing angles,

$$\frac{(\theta_L)_{i1}^{(\text{BP2})}}{(\theta_L)_{i1}^{(\text{BP1})}} \sim \epsilon^{-3}, \quad \frac{(\theta_L)_{i2}^{(\text{BP2})}}{(\theta_L)_{i2}^{(\text{BP1})}} \sim \epsilon^{-3}, \quad \frac{(\theta_L)_{i3}^{(\text{BP2})}}{(\theta_L)_{i3}^{(\text{BP1})}} \sim \epsilon^{-5}, \quad (4.18)$$

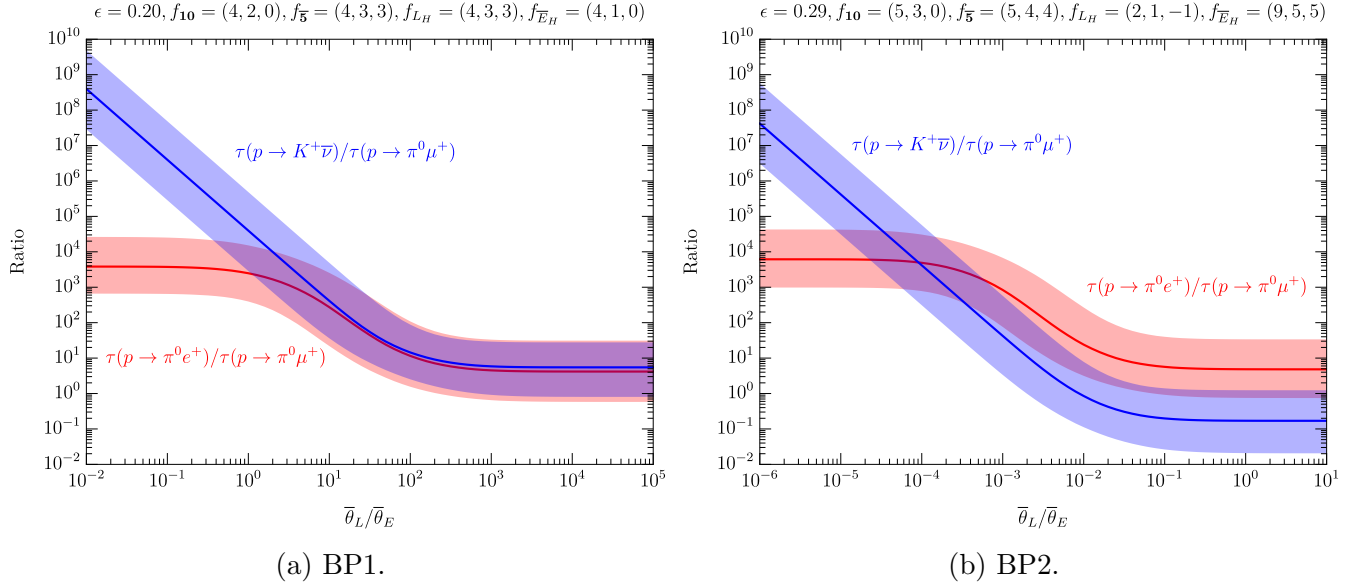


Figure 4: The lifetime ratios $\tau(p \rightarrow \pi^0 e^+)/\tau(p \rightarrow \pi^0 \mu^+)$ and $\tau(p \rightarrow K^+ \bar{\nu})/\tau(p \rightarrow \pi^0 \mu^+)$. Figure (a) and (b) show the result for BP1 and BP2, respectively.

(see Eq. (4.9)). Consequently, the branching fractions into the $\bar{\nu}_\tau$ modes are enhanced by a factor of ϵ^{-4} in BP2 compared to BP1, dominating the $\bar{\nu}$ modes in BP2.

In Fig. 4, we present the lifetime ratios $\tau(p \rightarrow \pi^0 e^+)/\tau(p \rightarrow \pi^0 \mu^+)$ and $\tau(p \rightarrow K^+ \bar{\nu})/\tau(p \rightarrow \pi^0 \mu^+)$ in the presence of both $\mathcal{O}^{(1)}$ and $\mathcal{O}^{(2)}$ decay operators. These ratios are expressed as functions of the ratio between lepton doublet and singlet mixing angles, $\bar{\theta}_L/\bar{\theta}_E$ as described in Eq. (4.11). Our analysis reveals that the proton typically decays into $\pi^0 \mu^+$ rather than $\pi^0 e^+$ across the entire range of $\bar{\theta}_L/\bar{\theta}_E$ in both benchmark points. Conversely, the behavior of the $K^+ \bar{\nu}$ mode varies depending on the benchmark point. In BP1, the proton is more likely to decay into $p \rightarrow \pi^0 \mu^+$ than $K^+ \bar{\nu}$ for all values of $\bar{\theta}_L/\bar{\theta}_E$. In BP2, however, there exists a range of $\bar{\theta}_L/\bar{\theta}_E$ where the proton is more likely to decay into $K^+ \bar{\nu}$. This behavior is influenced by $\bar{\theta}_L/\bar{\theta}_E$. Other $\bar{\nu}$ decay modes associated with different mesons, such as π , have similar behaviors to that of the $K^+ \bar{\nu}$ mode.

5 Conclusions and Outlooks

In this paper, we examined nucleon decay predictions within the fake GUT model based on $SU(5) \times U(2)_H$, incorporating the Froggatt-Nielsen (FN) mechanism. Our findings reveal that the flavor structure induced by the FN mechanism has a significant influence on nucleon decay modes. Due to the FN mechanism, each $SU(5)$ multiplet includes substantial contributions from the second and third generations of SM leptons. Consequently, nucleon decays into μ^+ and $\bar{\nu}_{\mu, \tau}$ become more probable. We identified the $p \rightarrow \pi^0 \mu^+$ mode as a prominent discovery channel. Moreover, the fake GUT model with the FN mechanism predicts a variety of nucleon decay channels, such as $p \rightarrow \pi^+ \bar{\nu}$, $n \rightarrow \pi^- \mu^+$, $n \rightarrow \pi^0 \bar{\nu}$, and $p \rightarrow K^+ \bar{\nu}$. This contrasts with the conventional GUT framework, where

the dominant mode is $p \rightarrow \pi^0 e^+$.

Our results demonstrate that the FN charge assignments substantially affect the branching fractions of nucleon decay. We have illustrated these effects using two benchmark points, BP1 and BP2, which show clear distinctions in the predicted decay modes. Notably, several nucleon decay modes fall within the detection capabilities of upcoming experiments. Our findings also motivate experimental searches for less-explored decay modes. Furthermore, they indicate that nucleon decay searches can provide insights not only into baryon number violation but also into the origin of the flavor structure.

Future work will include a comprehensive survey of FN charge assignments and the impact of the nucleon decay [39]. Additionally, we plan to extend this analysis to other models of flavor structures than the FN mechanism. It is also interesting to apply the present analysis on the FN mechanism to broader GUT models such as supersymmetric GUTs, where dimension-five operators may offer further insights into the impact of flavor symmetries on nucleon decay.

Acknowledgments

This work is supported by Grant-in-Aid for Scientific Research from the Ministry of Education, Culture, Sports, Science, and Technology (MEXT), Japan, 20H01895 and 20H05860 (S.S.), 21H04471 and 22K03615 (M.I.) and by World Premier International Research Center Initiative (WPI), MEXT, Japan. This work is supported by JST SPRING Grant Number JPMJSP2108 and ANRI fellowship (K.W.).

References

- [1] H. Georgi and S. L. Glashow, Phys. Rev. Lett. **32**, 438 (1974).
- [2] H. Georgi, H. R. Quinn, and S. Weinberg, Phys. Rev. Lett. **33**, 451 (1974).
- [3] A. J. Buras, J. R. Ellis, M. K. Gaillard, and D. V. Nanopoulos, Nucl. Phys. B **135**, 66 (1978).
- [4] S. Navas *et al.* (Particle Data Group), Phys. Rev. D **110**, 030001 (2024).
- [5] A. Takenaka *et al.* (Super-Kamiokande), Phys. Rev. D **102**, 112011 (2020), arXiv:2010.16098 [hep-ex] .
- [6] K. Abe *et al.* (Hyper-Kamiokande), (2018), arXiv:1805.04163 [physics.ins-det] .
- [7] F. An *et al.* (JUNO), J. Phys. G **43**, 030401 (2016), arXiv:1507.05613 [physics.ins-det] .
- [8] B. Abi *et al.* (DUNE), Eur. Phys. J. C **81**, 322 (2021), arXiv:2008.12769 [hep-ex] .

- [9] M. Ibe, S. Shirai, M. Suzuki, and T. T. Yanagida, Phys. Rev. D **100**, 055024 (2019), arXiv:1906.02977 [hep-ph] .
- [10] M. Ibe, S. Shirai, M. Suzuki, K. Watanabe, and T. T. Yanagida, JHEP **07**, 087 (2022), arXiv:2205.01336 [hep-ph] .
- [11] L. J. Hall and K. Harigaya, JHEP **10**, 130 (2018), arXiv:1803.08119 [hep-ph] .
- [12] L. J. Hall and K. Harigaya, JHEP **11**, 033 (2019), arXiv:1905.12722 [hep-ph] .
- [13] H. Fritzsch and Z.-z. Xing, Prog. Part. Nucl. Phys. **45**, 1 (2000), arXiv:hep-ph/9912358 .
- [14] G. Altarelli and F. Feruglio, Rev. Mod. Phys. **82**, 2701 (2010), arXiv:1002.0211 [hep-ph] .
- [15] C. D. Froggatt and H. B. Nielsen, Nucl. Phys. B **147**, 277 (1979).
- [16] G. 't Hooft, C. Itzykson, A. Jaffe, H. Lehmann, P. K. Mitter, I. M. Singer, and R. Stora, eds., *Recent Developments in Gauge Theories. Proceedings, Nato Advanced Study Institute, Cargese, France, August 26 - September 8, 1979*, Vol. 59 (1980).
- [17] P. Minkowski, Phys. Lett. B **67**, 421 (1977).
- [18] T. Yanagida, Conf. Proc. C **7902131**, 95 (1979); T. Yanagida, Phys. Rev. D **20**, 2986 (1979).
- [19] M. Gell-Mann, P. Ramond, and R. Slansky, Conf. Proc. C **790927**, 315 (1979), arXiv:1306.4669 [hep-th] .
- [20] S. L. Glashow, NATO Sci. Ser. B **61**, 687 (1980).
- [21] R. N. Mohapatra and G. Senjanovic, Phys. Rev. Lett. **44**, 912 (1980).
- [22] J. Sato and T. Yanagida, Phys. Lett. B **430**, 127 (1998), arXiv:hep-ph/9710516 .
- [23] K. S. Babu, A. Khanov, and S. Saad, Phys. Rev. D **95**, 055014 (2017), arXiv:1612.07787 [hep-ph] .
- [24] R. L. Workman *et al.* (Particle Data Group), PTEP **2022**, 083C01 (2022).
- [25] D. Buttazzo, G. Degrandi, P. P. Giardino, G. F. Giudice, F. Sala, A. Salvio, and A. Strumia, JHEP **12**, 089 (2013), arXiv:1307.3536 [hep-ph] .
- [26] K. G. Chetyrkin, B. A. Kniehl, and M. Steinhauser, Phys. Rev. Lett. **79**, 2184 (1997), arXiv:hep-ph/9706430 .
- [27] N. Nagata and S. Shirai, JHEP **03**, 049 (2014), arXiv:1312.7854 [hep-ph] .
- [28] L. F. Abbott and M. B. Wise, Phys. Rev. D **22**, 2208 (1980).

- [29] T. Nihei and J. Arafune, Prog. Theor. Phys. **93**, 665 (1995), arXiv:hep-ph/9412325 .
- [30] J.-S. Yoo, Y. Aoki, P. Boyle, T. Izubuchi, A. Soni, and S. Syritsyn, Phys. Rev. D **105**, 074501 (2022), arXiv:2111.01608 [hep-lat] .
- [31] Y. Aoki, T. Izubuchi, E. Shintani, and A. Soni, Phys. Rev. D **96**, 014506 (2017), arXiv:1705.01338 [hep-lat] .
- [32] M. Machacek, Nucl. Phys. B **159**, 37 (1979).
- [33] S. Weinberg, Phys. Rev. Lett. **43**, 1566 (1979).
- [34] K. Abe *et al.* (Super-Kamiokande), Phys. Rev. Lett. **113**, 121802 (2014), arXiv:1305.4391 [hep-ex] .
- [35] K. Kobayashi *et al.* (Super-Kamiokande), Phys. Rev. D **72**, 052007 (2005), arXiv:hep-ex/0502026 .
- [36] R. Matsumoto *et al.* (Super-Kamiokande), Phys. Rev. D **106**, 072003 (2022), arXiv:2208.13188 [hep-ex] .
- [37] K. Abe *et al.* (Super-Kamiokande), Phys. Rev. D **90**, 072005 (2014), arXiv:1408.1195 [hep-ex] .
- [38] N. Taniuchi *et al.* (Super-Kamiokande), (2024), arXiv:2409.19633 [hep-ex] .
- [39] M. Ibe, S. Shirai, and K. Watanabe, to appear.